

Robust OOD Graph Learning via Mean Constraints and Noise Reduction

Yang Zhou
Independent Researcher
China
zz199999999@outlook.com

Xiaoning Ren
University of Science and Technology of China
Hefei, China
hnurxn@mail.ustc.edu.cn

Abstract

Graph Out-of-Distribution (OOD) classification often suffers from sharp performance drops, particularly under category imbalance and structural noise. This work tackles two pressing challenges in this context: (1) the underperformance of minority classes due to skewed label distributions, and (2) their heightened sensitivity to structural noise in graph data. To address these problems, we propose two complementary solutions. First, Constrained Mean Optimization (CMO) improves minority class robustness by encouraging similarity-based instance aggregation under worst-case conditions. Second, the Neighbor-Aware Noise Reweighting (NNR) mechanism assigns dynamic weights to training samples based on local structural consistency, mitigating noise influence. We provide theoretical justification for our methods, and validate their effectiveness with extensive experiments on both synthetic and real-world datasets, showing significant improvements in Graph OOD generalization and classification accuracy. The code for our method is available at: <https://anonymous.4open.science/r/CMO-NNR-2F30>.

ACM Reference Format:

Yang Zhou and Xiaoning Ren. 2025. Robust OOD Graph Learning via Mean Constraints and Noise Reduction. In . ACM, New York, NY, USA, 8 pages. <https://doi.org/10.1145/nnnnnnnn.nnnnnnnn>

1 Introduction

Graph-based learning has become a fundamental approach for modeling relational data in diverse domains, such as social networks, biological systems, and recommendation platforms[5, 8, 24, 26, 27]. However, in practical applications, graphs collected from different environments often exhibit distribution shifts due to variations in structural patterns, feature distributions, or labeling rules. These shifts pose significant challenges to model generalization, leading to the emergence of Graph OOD research as a growing field focused on improving robustness across graph distribution shifts[12, 13, 19, 21].

Recently, there has been a rise in Graph OOD research[2, 6, 10, 11, 22, 23, 25] that aim to improve generalization performance on complex distribution shifts. For instance, GALA[2] use contrastive learning to maximize intra-class mutual information on different environments to learn causally invariant representations

Permission to make digital or hard copies of all or part of this work for personal or classroom use is granted without fee provided that copies are not made or distributed for profit or commercial advantage and that copies bear this notice and the full citation on the first page. Copyrights for components of this work owned by others than the author(s) must be honored. Abstracting with credit is permitted. To copy otherwise, or republish, to post on servers or to redistribute to lists, requires prior specific permission and/or a fee. Request permissions from permissions@acm.org.
Conference'17, Washington, DC, USA

© 2025 Copyright held by the owner/author(s). Publication rights licensed to ACM.
ACM ISBN 978-x-xxxx-xxxx-x/YYYY/MM
<https://doi.org/10.1145/nnnnnnnn.nnnnnnnn>

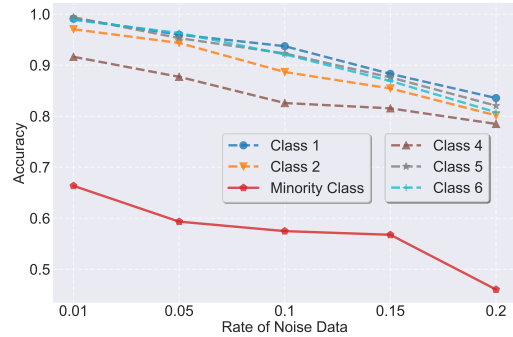


Figure 1: Accuracy for each category in different noise data rate

for graph. From another perspective, DIR[25] and IGM[10] directly handle data shifts directly by employing Empirical Risk Minimization (ERM), which is implemented by designing new environments.

In this work, we identified a Graph OOD issue that has been overlooked by existing research, i.e., *the performance of minority classes decreases caused by imbalanced and noisy data*. As shown in Figure 1, the accuracy of the minority class is lower and will be exacerbated as noise increases.

Class imbalance is an important challenge in Graph OOD learning, where distribution shifts are amplified by uneven sample sizes across classes. Under such imbalance, the model tends to overfit the majority classes while failing to extract stable patterns from minority classes, weakening its performance in minority class predictions[1, 20]. Noisy data is another factor that exacerbates Graph OOD generalization, as noise negatively impacts model performance. It disrupts the extraction of consistent representations and disproportionately affects minority classes, whose limited samples are more sensitive to corrupted information, leading to further degradation[3, 7].

To address these challenges, we propose two methods: CMO and NNR. CMO focuses on solving the class imbalance problem. It adds a constraint about the mean value of graph features during the update process, helping the model identify the worst-performing cases more effectively than traditional Distributionally Robust Optimization (DRO) methods. As a result, CMO balances the learning process and improves performance across all classes. NNR aims to reduce the impact of noisy data. During training, it assigns lower weights to samples likely to be noisy. To estimate the likelihood of each instance being noise, NNR counts the number of same-class neighbors within a certain distance. Fewer same-class neighbors suggest a higher probability of noise. By reducing the influence of these suspected noisy samples, especially in small classes, NNR

helps the model focus on more reliable data. This improves generalization and enhances robustness against noise.

Our contributions can be summarized as follows:

We propose a novel constrained optimization method for updating q , improving stability and adaptability in OOD settings.

We introduce a noise-aware loss weighting strategy that reduces the influence of noisy data, enhancing model generalization.

We provide a comprehensive theoretical analysis of both methods, demonstrating their effectiveness in addressing OOD challenges.

We design synthetic datasets that simulate real-world scenarios to analyze the impact of data imbalance and noise, and conduct comprehensive evaluations on both synthetic and real-world datasets[9] to verify the effectiveness of our proposed methods.

2 Preliminaries

We consider a graph classification problem in a cross-environment setting[2].

ASSUMPTION 1. *In each environment e , every graph G_i belonging to class c is assumed to consist of two components, each of which is modeled as a Gaussian distribution:*

- **Invariant feature** $x_{inv} \sim \mathcal{N}(\mu_c, \sigma^2 I)$, which reflects the inherent semantics associated with class c . This feature is common across environments and captures the casual representation of the class.
- **Spurious feature** $x_{spu} \sim \mathcal{N}(\mu_c^e, \sigma^2 I)$, which captures the environment-specific bias in e .

Each class c is modeled by a Gaussian distribution with mean vector μ_c , and the environment-specific spurious feature has a Gaussian distribution with mean μ_c^e for each environment e .

As shown in 1, the performance of the minority class is often worse than that of the other classes. This poorer performance thus often causes a higher loss value, indicating that the model is struggling to make accurate predictions for these minority categories. Since loss is directly related to the model's prediction error, a higher loss suggests that the minority class is more likely to be classified as part of the "worst-case" scenarios during training.

DRO algorithms aim to identify and optimize for the worst-case scenarios[18]. These methods enhance the model's generalization ability by focusing on the most challenging cases, which often include high-loss instances. Given this, we propose applying DRO algorithms as foundation to address the performance gap in the minority class.

2.1 DRO Algorithms

Traditional DRO algorithms usually generate datasets that satisfy a constraint in the training data, and optimize the worst-performing data in order to improve the generalization ability of the model. Typically, the optimization objective is:

$$\min_{f \in \mathcal{F}} \{R(f, q)\} \quad (1)$$

where the objective function $R(f, q)$ is defined as:

$$R(f, q) \equiv \max_{q \in \Delta_m} \sum_{i=0}^n q_i \mathbb{E}_{(x, y) \sim P(X, Y)} [\ell(f(x), y)] \quad (2)$$

and the constraint is:

$$\text{s.t. } D(Q \| P) < \rho, \quad (3)$$

$$Q = \left\{ \sum_{i=1}^n q_i P_i \mid q \in \Delta_m \right\} \quad (4)$$

Q represents the mixture of the test data distribution, $P = \sum_{i=1}^n P_i$ is the training data distribution, and q_i is the weight of each group P_i .

The constraint $D(Q \| P) < \rho$ aims to ensure that the newly generated dataset maintains an appropriate difference from the original training data, thereby enhancing the model's generalization ability while avoiding significant deviation from the original data distribution.

2.2 Divergence

In this study, we focus on the f -divergences from the Cressie-Read family[4], defined by the parameter k . Specifically, we define the function:

$$f_k(t) = k(k-1)t^k - kt + k - 1, \quad (5)$$

and construct the divergence:

$$D_k(Q \| P) = \int f_k \left(\frac{dP}{dQ} \right) dP. \quad (6)$$

When $k = 1$, this divergence reduces to the KL divergence. When $k = 2$, it becomes the Chi-squared divergence.

3 Methods

In this section, we present two parallel methods (shown in 2) designed to address the poor performance of minority class due to data imbalance problem and the impact of noisy data in Graph Neural Networks (GNNs).

3.1 Constrained Mean Optimization (CMO)

Traditional DRO algorithms typically maximize the loss function to find the worst-performing distribution Q . However, this process ignores an important prior: for classification problems, smaller distributional differences between classes often lead to worse classification performance. For example, suppose we are classifying Alaskan Malamutes, Siberian Huskies, and cats. In this case, more worst-case scenarios are likely to occur between Alaskan Malamutes and Siberian Huskies, as these two breeds have more similar representations compared to cats. This class similarity is a crucial prior knowledge that can be used to improve the DRO algorithms.

To effectively utilize the prior information of classification problems, we introduce a class-wise distribution similarity constraint, making the optimization objective:

$$\min_{f \in \mathcal{F}} \{R(f, q)\}, \quad (7)$$

where $R(f, q)$ is still defined as:

$$R(f, q) \equiv \max_{q \in \Delta_m} \sum_{i=0}^n q_i \mathbb{E}_{(x, y) \sim P(X, Y)} [\ell(f(x), y)], \quad (8)$$

and the updated constraint is:

$$\text{s.t. } D(Q \| P) < \rho_1, \Delta(Q) < \rho_2. \quad (9)$$

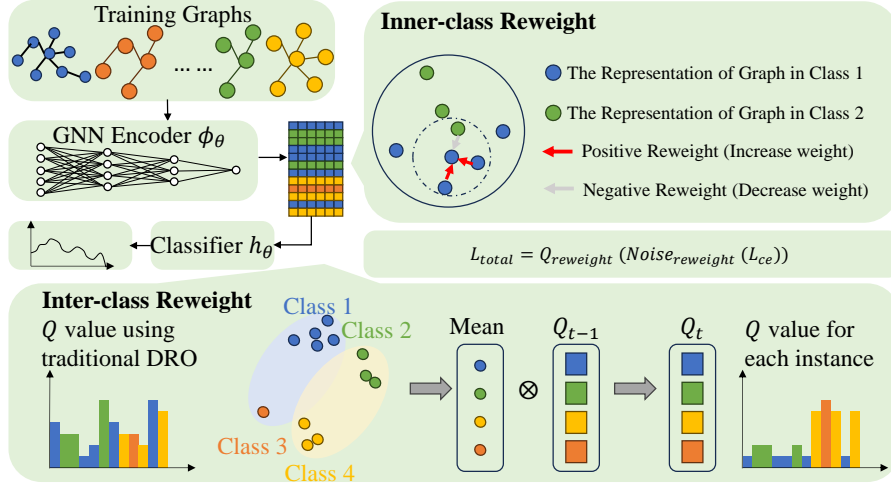


Figure 2: Our framework is composed of CMO and NNR, corresponding to inter-class and inner-class reweighting, respectively.

$$\Delta(Q) = \sum_{i=1}^n \sum_{j=i+1}^n (\mu(Q_i) - \mu(Q_j))^2. \quad (10)$$

$\Delta(Q)$ represents the sum of squares of the feature differences between classes.

To solve the optimization problem with these constraints, we use the Lagrange multiplier method to construct the Lagrangian dual function:

$$L = \sum_{i=0}^n q_i \mathbb{E}_{(x,y) \sim P(X,Y)} [\ell(f(x), y)] - \lambda_1 (D(Q||P) - \rho_1) - \lambda_2 (\Delta(Q) - \rho_2). \quad (11)$$

Let θ represent the parameters of the model $f(x)$, and the update formulas for θ and q are:

$$q^{(t+1)} = q^{(t)} + \eta_q \nabla_q L, \quad \theta^{(t+1)} = \theta^{(t)} - \eta_\theta \nabla_\theta L, \quad (12)$$

where η_q and η_θ are the update step sizes for q and θ , respectively.

3.2 Convergence Analysis

In this section, we prove that by choosing appropriate learning rates η_θ and η_q , the proposed optimization method can ensure the convergence of the parameters θ and q for both convex and non-convex loss functions.

DEFINITION 1. A mapping $f : X \rightarrow \mathbb{R}^m$ is L -Lipschitz continuous if for any $x, y \in X$,

$$\|f(x) - f(y)\| \leq L\|x - y\|. \quad (13)$$

DEFINITION 2. A function $f : X \rightarrow \mathbb{R}$ is L -smooth if it is differentiable on X and the gradient ∇f is G -Lipschitz continuous, i.e.,

$$\|\nabla f(x) - \nabla f(y)\| \leq G\|x - y\| \quad \text{for all } x, y \in X. \quad (14)$$

ASSUMPTION 2. We assume that the loss function satisfies the above two properties (1 and 2).

Convex Loss Functions For convex loss functions, we estimate the convergence rate based on the expected number of stochastic gradient updates. To achieve a duality gap of ϵ [16], the optimal

convergence rate for solving stochastic min-max problems $O(1/\epsilon^2)$ assuming the problem is convex-concave. The duality gap for the pair $(\tilde{\theta}, \tilde{q})$ is

$$\max_{q \in \Delta_m} R(\tilde{\theta}, q) - \min_{\theta \in \Theta} R(\theta, \tilde{q}). \quad (15)$$

In cases of strong duality, the pair $(\tilde{\theta}, \tilde{q})$ is considered optimal when the duality gap is zero. Our method is shown to achieve the optimal rate of $O(1/\epsilon^2)$ in this setting. Consider the problem in 11.

THEOREM 1. Assuming the loss function is convex and Assumption 2 is satisfied. Let Θ be bounded by R_θ , with $\mathbb{E} [\|\nabla_\theta R(\theta, q)\|_2^2] \leq \hat{G}_\theta^2$ and $\mathbb{E} [\|\nabla_q R(\theta, q)\|_2^2] \leq \hat{G}_q^2$, our method satisfies:

$$\mathbb{E} \left[\max_{q \in \Delta_m} R(\theta^T, q) - \min_{\theta \in \Theta} R(\theta, q^T) \right] \leq 2G_q + 2\|R_\theta\|_2 G_\theta + \frac{1}{\sqrt{T}} \left(\mathbb{E} [\|\theta^1 - \theta\|_2] G_\theta \right) + \frac{1}{\sqrt{T}} \left(\mathbb{E} [\|q^1 - q\|_2] G_q \right) \quad (16)$$

The proof of 1 is detailed in Supplementary material. This inequality shows that the expectation of the dual gap monotonically decreases as the number of iterations T increases, converging at a rate of $O(1/T)$, thus ensuring the convergence of the optimization process under convex loss functions.

Non-Convex Loss Functions For non-convex loss.

THEOREM 2. Based on Assumption 2

$$\lim_{T \rightarrow \infty} \sum_{t=1}^T \mathbb{E} [\|\nabla_\theta L(\theta_t, q_t)\|] = 0. \quad (17)$$

The proof of 2 is detailed in Supplementary material. This result shows that as the number of iterations increases, the cumulative gradient norm tends to zero, ensuring that in the case of non-convex losses, the algorithm can find a stationary point, guaranteeing overall convergence.

3.3 Neighbor-Aware Noise Reweighting (NNR)

In DRO algorithms, the model typically focuses on optimizing the worst-performing cases, which often leads to overemphasis on noisy data. **This can cause a significant issue, as noisy data tends to negatively impact the model's performance by introducing misleading patterns.** Noisy data usually manifests as poor performance in the ideal model, and traditional Graph OOD methods, as described in 2, tend to prioritize such poorly performing data during training. This causes disturbance in the training process, leading the model to deviate from the true target. **To resolve this issue, we propose a neighbor-based weight adjustment method,** which aims to reduce the influence of noisy data by adjusting the weight based on data similarity.

Basic Idea: According to Assumption 1, since the invariant features of class c follow a Gaussian distribution $x_{inv} \sim \mathcal{N}(\mu_c, \sigma^2 I)$, a sample with more neighbors sharing similar labels is more likely to be reliable and consistent with the true distribution, thus assigned a higher weight. Conversely, if there are fewer such neighboring instances, the sample is considered more likely to be noisy and is assigned a lower weight.

Normalization: Since imbalanced data distribution is very common in the Graph OOD problem, it is necessary to normalize the number of the same data in the neighborhood to eliminate the impact of different class sizes.

Implementation Details: First, for each graph data G_i , we calculate the "same" neighbors within a certain distance, denoted as $N_{hm}(G_i)$. Then, for each sample G_i , we calculate the total number of graph instances in training progress, denoted as $N_{sum}(G_i)$. The weight w_i of data G_i is defined as:

$$w_i = \frac{N_{hm}(G_i)}{N_{sum}(G_i)}. \quad (18)$$

And, this weight w_i is applied to the loss calculation for graph G_i , resulting in the weighted loss function:

$$\ell_i = w_i \ell_i^{raw}. \quad (19)$$

This method helps to reduce the contribution of noisy data, thereby improving the robustness of the model.

3.4 OOD Generalization Error Bound

In this section, we derive an OOD generalization error bound to demonstrate that NNR effectively minimizes OOD error. To achieve this, we adopt a PAC-Bayesian framework, following the approach proposed by Ma et al. (2021)[14]. The total set of graphs in the environment e is denoted by G^e , with training and test sets represented as G_{tra}^e and G_{te}^e , respectively.

3.4.1 Graph Embedding and Global Features.

DEFINITION 3 (GRAPH EMBEDDING). For each graph G_i , we obtain an embedding $g_i \in \mathbb{R}^d$ via global pooling (e.g., Readout) from a GNN. The classification function $f: \mathbb{R}^d \rightarrow \mathbb{R}^c$ satisfies the Lipschitz continuity condition:

$$\|f(g_i) - f(g_j)\| \leq C \|g_i - g_j\|, \quad (20)$$

where L is the Lipschitz constant, ensuring that nearby embeddings yield similar classification outputs.

DEFINITION 4 (FEATURE DISTANCE AGGREGATION). To characterize the difficulty of cross-environment generalization, we define the graph embedding distance between the test environment G_{te}^e and the training environment G_{tra}^e as:

$$\Gamma = \max_{G_j \in G_{te}^e} \min_{G_i \in G_{tra}^e} \|g_i - g_j\|_2. \quad (21)$$

A larger Γ indicates that test graphs are farther from training graphs in the embedding space, which increases the generalization difficulty.

3.4.2 Margin Loss and Classifier Constraints.

DEFINITION 5 (MARGIN LOSS). The graph classification margin loss function for environment e is defined as:

$$L_Y^e(h) = \frac{1}{|G^e|} \sum_{G_i \in G^e} \mathbb{I} \left[h(g_i)[y_i] \leq \gamma + \max_{c \neq y_i} h(g_i)[c] \right], \quad (22)$$

where $h: \mathbb{R}^d \rightarrow \mathbb{R}^c$ is the classifier, γ is the margin threshold, and \mathbb{I} is the indicator function.

ASSUMPTION 3 (EQUAL-SIZED AND DISJOINT NEAR SETS). For any $0 < m \leq M$, assume the near sets of each graph $G_i \in G_{tra}$ with respect to G_{te} are disjoint and have the same size $s_m \in \mathbb{N}^+$.

ASSUMPTION 4 (CROSS-ENVIRONMENT EMBEDDING COVERAGE). For any test environment e_{test} , there exists a coverage radius Γ such that for every training graph $G_i \in G_{tra}^e$, the neighboring test graph set

$$N_\Gamma(G_i) = \{G_j \in G_{te}^e \mid \|g_i - g_j\|_2 \leq \Gamma\} \quad (23)$$

is non-empty. g_i denotes as a Readout function. Additionally, we assume: There exists a constant $s_e > 0$ such that for most training graphs, $|N_\Gamma(G_i)| \geq s_e$. The neighboring sets $N_\Gamma(G_i)$ should exhibit minimal overlap to better characterize training sample coverage.

ASSUMPTION 5 (CONCENTRATED EXPECTED LOSS DIFFERENCE). Let P be a distribution over the hypothesis space H , defined by sam-

pling the vectorized MLP parameters from $\mathcal{N}(0, \sigma^2 I)$ for $\sigma^2 \leq \frac{(\frac{\gamma}{8})^2}{2b(\lambda|G_{tra}| + \ln 2bL)}$. For any L -layer GNN classifier $h \in H$ with model parameters W_1^h, \dots, W_L^h , define $T_h := \max_{l=1, \dots, L} \|W_l^h\|_2$. Assume that there exists some $0 < \alpha < \frac{1}{4}$ such that

$$\mathbb{P}_{h \sim P} \left(A > B \mid T_h^L \Gamma > \frac{\gamma}{8} \right) \leq \exp(-|G_{te}|^{2\alpha}). \quad (24)$$

$$A = L_{\gamma/4}^{e_{test}}(h) - L_{\gamma/2}^{e_{train}}(h) \quad \text{and} \quad B = |G_{tra}|^{-\alpha} + \text{CGT}$$

THEOREM 3. For any classifier $h \in H$ and environment e^{test} , under the Assumption 3 4 5, when the number of training graphs $|G_{tra}|$ is sufficiently large, there exists a constant $\alpha \in (0, 1/4)$ such that with probability at least $1 - \delta$, the following holds:

$$L(e^{test}) \leq L(e^{train}) + O \left(\frac{1}{|G_{tra}^e|} \sum_{i \in G_{tra}^e} \frac{1}{|G_{te}^e|} \sum_{j \in G_{te}^e} \sum_{c=1}^C \sum_{c' \neq c} [Term_1 + Term_2 + Term_3] \right) \quad (25)$$

$$Term_1 = \frac{1}{\sigma^2} \left((g_j^T w_j - g_i^T w_i)(\mu_{c'} - \mu_c) \right) \quad (26)$$

$$\text{Term}_2 = \frac{1}{2\sigma^2} \left(w_j^2 (f(\mu^{test})) - w_i^2 (f(\mu^{train})) \right) \quad (27)$$

$$f(\mu) = \|\mu_c\|_2^2 - \|\mu_{c'}\|_2^2 \quad (28)$$

$$\text{Term}_3 = \frac{1}{2\sigma^2} \left((w_j^2 - w_i^2) (\|\mu_c\|_2^2 - \|\mu_{c'}\|_2^2) \right) \quad (29)$$

The detail of Theorem 3 can be found in Supplementary material. μ_c and $\mu_{c'}$ denote the class centers of classes c and c' , respectively. g_i and g_j are the readout values of samples i and j from the training set G_{tra}^e and test set G_{te}^e , respectively. w_i and w_j are the corresponding weights of samples g_i and g_j . $|G_{tra}^e|$ and $|G_{te}^e|$ represent the sizes of the training and test sets for environment e , and C is the total number of classes. Based on the above 25, the error bound can be decomposed into three distinct terms.

- (1) **Class Center Differences and Weighted Distance:** Measures the difference between class centers $\|\mu_{c'} - \mu_c\|_2$ and the weighted distance $\|g_j^T w_j - g_i^T w_i\|_2$ between samples, with w_i and w_j as sample weights, combining class centrality and sample distances.
- (2) **Cross-Environment Feature Mean Differences:** Calculates the differences in feature means $\|\mu_{c, test}\|_2^2 - \|\mu_{c', test}\|_2^2$ between the training and test environments, highlighting discrepancies in feature distributions.
- (3) **Weighted Distribution of Different-Class Neighbor Ratios:** Assesses the weighted differences in feature distributions of different classes based on different-class neighbor ratios across environments.

Based on the formulas, we can indirectly adjust the weight w through the parameter Γ , thereby controlling the model's Generalization Error Bound.

4 Experiment

In this section, we provide a detailed explanation of the experimental setup and present a subset of the results (due to space limitations). Additional experimental results can be found in the Supplementary material.

4.1 Dataset

To evaluate the effectiveness of the proposed method, we conduct experiments in both synthetic datasets and real-world datasets[9].

Synthetic Datasets We have constructed a synthetic dataset consisting of two parts: invariant features, which determine the true label, and spurious features. To simulate real-world noise, we introduce two key parameters:

- (1) **Noise Ratio (α):** The probability that invariant features do not match the true label, with a proportion of samples having their labels randomly assigned. The noise ratio varies across 0.01, 0.05, 0.1, 0.15, 0.2.
- (2) **Correlation Strength (β):** The relationship between invariant and spurious features. When $\beta = 1$, spurious features are fully determined by the invariant features.

The dataset, which we have synthesized, contains six classes: classes 1, 2, 4, 5, and 6 each with 3000 samples, and class 3 with 300 samples. Each class has 1000 samples for validation and testing. Various combinations of noise ratios and correlation strengths produce different dataset variations, which we use to test our model.

Real-world Dataset In addition to the synthetic dataset, we also conducted experiments on real-world datasets[9] to verify the generalization ability of our method. The information for these three datasets is shown in 2.

4.2 Baseline Methods

For our experiments, we selected a simple 3-layer Graph Neural Network (GNN) as the backbone model. As for the baseline methods, we chose the most commonly used ERM approach along with several other advanced techniques. These include:

- **ERM[17]:** Standard empirical risk minimization on training data.
- **CVaR[28]:** DRO method minimizing loss over the worst α fraction of samples to improve tail performance.
- **Chisq[28]:** DRO method using χ^2 -divergence to reweight samples, emphasizing high-loss cases.
- **CVaR_doro[28]:** CVaR extension with outlier robustness by filtering the top ϵ high-loss samples.
- **Chisq_doro[28]:** Chisq extension with outlier robustness by ignoring some high-loss samples.
- **CVaR_group[28]:** CVaR-based method minimizing worst-case group risk using known group information.
- **Group[18]:** DRO method minimizing worst-case loss across predefined groups.
- **Gradient[15]:** DRO method minimizing worst-case loss based on group gradients.
- **Variant:** DRO method minimizing worst-case loss based on group variance.

To evaluate the performance of our proposed methods, we use the following configurations: **ERM+NNR**, **ERM+CMO-KL**, **ERM+CMO-Chi**, **ERM+NNR+CMO-KL**, and **ERM+NNR+CMO-Chi**.

4.3 Evaluation Metric

The primary evaluation metric used in our experiments is **accuracy**, defined as the proportion of correctly classified samples out of the total number of samples. In addition to the overall accuracy, we focus on the accuracy of the **minority class**, as well as the overall accuracy, to assess the model's performance in handling imbalanced data and noisy environments.

4.4 Parameter Settings

We set the batch size to 32 and the number of epochs to 400. The learning rate is initialized at 0.001. We also perform experiments using random seeds 1, 2, 3, 4, and 5. The pooling method used is mean pooling, and the embedding dimension is set to 32.

4.5 Overall Performance

As shown in 1, our proposed methods, CMO and NNR, demonstrate clear advantages as the noise ratio increases. CMO consistently improves performance under different noise levels, showing its robustness to class imbalance. NNR further enhances the upper bound of model accuracy, reaching 80.2% and 79.8% when combined with CMO-KL and CMO-Chi, which surpass the best baseline results (71.6% and 74.7%, respectively). This indicates that NNR effectively

Method	Minority Class Accuracy (Average%)		Minority Class Accuracy (Max%)		All Classes Average Accuracy (Average%)	
	0.15	0.2	0.15	0.2	0.15	0.2
ERM	54.9 ±0.1	53.6 ±0.4	60.3	63.1	80.9	76.7
ERM+NNR	<u>70.1</u> ±0.5	58.6 ±0.6	83.6	73.4	<u>81.1</u>	<u>77.0</u>
ERM+CMO-KL	<u>67.8</u> ±0.5	<u>62.8</u> ±0.5	81.5	71.6	80.9	<u>76.7</u>
ERM+CMO-Chi	67.5 ±0.6	<u>61.6</u> ±0.5	<u>85.0</u>	<u>74.7</u>	81.0	76.7
ERM+NNR+CMO-KL	<u>67.9</u> ±0.8	<u>59.3</u> ±0.8	<u>85.6</u>	<u>80.2</u>	<u>81.1</u>	75.5
ERM+NNR+CMO-Chi	67.2 ±0.3	58.5 ±0.7	<u>85.0</u>	<u>79.8</u>	<u>81.1</u>	75.8
CVaR	55.0 ±0.1	54.0 ±0.2	60.3	62.7	81.0	<u>76.8</u>
Chisq	57.3 ±0.4	54.4 ±0.3	72.3	62.8	81.1	76.7
CVaR_doro	55.1 ±0.2	52.0 ±0.3	64.8	59.8	80.9	76.4
Chisq_doro	55.6 ±0.2	53.0 ±0.3	67.7	61.3	80.8	76.6
CVaR_group	55.5 ±0.2	53.0 ±0.2	69.9	62.3	80.9	76.7
Variant	53.0 ±0.6	53.7 ±1.0	67.7	69.0	78.1	74.0
Group	53.9 ±0.2	52.4 ±0.3	61.4	63.1	80.9	76.5
Gradient	56.6 ±0.1	52.0 ±0.3	63.8	60.2	81.0	76.4

Table 1: Performance Results for Various Methods on Synthetic Datasets (In the table above, for the columns 'Minority Class Accuracy (Average%)' and 'All Classes Average Accuracy (Average%)', entries without a variance annotation indicate a variance of 0.0%. The blue single underline denotes the first place, the orange dotted underline indicates the second place, and the yellow double underline represents the third place.)

	Train		Validation		Test	
	Class 1	Class 2	Class 1	Class 2	Class 1	Class 2
Assay	68	8325	67	4564	305	4338
Scaffold	82	8399	76	4568	277	4194
Size	38	5285	76	4587	289	4379

Table 2: Information about the real-world dataset for training, validation, and testing for drugood_lbp_core_ki.

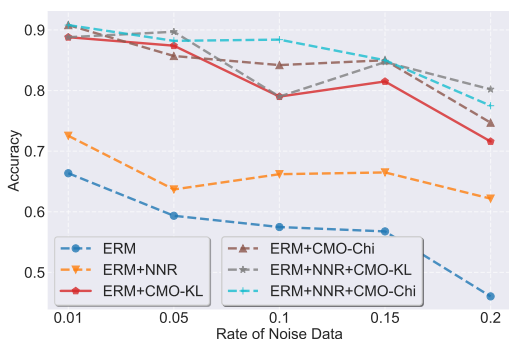


Figure 3: The performance of the minority class with respect to different noise rates on synthetic datasets.

reduces the influence of noisy data and helps the model capture more reliable patterns.

On real-world datasets 3, our methods consistently achieve superior performance, particularly for the minority class. As shown in 4, we significantly improve the upper-bound accuracy of minority groups across all tasks, reaching up to 47.2% in Assay, 34.9% in Scaffold, and 48.0% in Size. This demonstrates the strong potential

of our approach in handling challenging, imbalanced real-world scenarios. Although we observe increased variance, this is expected due to the absence of dataset-specific weighting strategies during evaluation. Nevertheless, the notable performance gains clearly outweigh this trade-off, confirming the robustness and adaptability of our methods.

However, NNR slightly reduces average accuracy and increases variance (about 0.2%-0.3%), suggesting that its noise estimation may occasionally misclassify clean samples, leading to instability. In the Scaffold dataset, NNR alone (ERM+NNR) achieves limited gains (6.9%±0.2%) as the dataset's inherent structure reduces the presence of outliers, limiting the effect of noise suppression.

Overall, these results demonstrate that CMO and NNR provide complementary benefits. CMO offers stable improvements across various settings by addressing class imbalance, while NNR enhances robustness against noise, particularly under challenging conditions with high noise levels.

4.6 Ablation Study

In this section, we conduct ablation experiments to assess the impact of different components on our model's performance. As shown in 1, our full model (NNR + CMO-KL/CMO-Chi) consistently achieves the best results across both synthetic and real-world datasets. This demonstrates the effectiveness of our proposed methods, with NNR mitigating noise and CMO enhancing robustness. Furthermore, as illustrated in 5, our method effectively identifies and prioritizes the worst-performance cases, particularly the minority class. The minority class exhibits a significantly higher Q value than other classes, far exceeding the initial weight baseline (yellow dashed line), highlighting the model's focused optimization on harder cases. **These results validate the complementary benefits of NNR and CMO, where noise suppression and adaptive reweighting jointly contribute to performance gains.**

Method	drugood_lbap_core_ki_assay(Average%)		drugood_lbap_core_ki_scaffold(Average%)		drugood_lbap_core_ki_size(Average%)	
	Class 1	Class 2	Class 1	Class 2	Class 1	Class 2
ERM	13.0 ±0.4	<u>96.2</u>	6.3 ±0.1	<u>97.6</u>	14.9 ±0.6	97.2
ERM+NNR	12.9 ±0.3	95.7	6.9 ±0.2	96.1	13.1 ±0.6	<u>97.8</u>
ERM+CMO-KL	<u>19.3</u> ±0.7	90.6 ±0.2	8.5 ±0.4	96.1 ±0.1	19.9 ±0.9	94.6 ±0.1
ERM+CMO-Chi	19.2 ±1.0	90.7 ±0.3	10.1 ±0.4	95.2 ±0.1	19.1 ±0.8	94.5 ±0.1
ERM+NNR+CMO-KL	<u>21.2</u> ±0.6	89.7 ±0.3	<u>15.2</u> ±0.7	92.6 ±0.3	<u>27.4</u> ±0.8	91.3 ±0.2
ERM+NNR+CMO-Chi	<u>21.2</u> ±0.9	90.6 ±0.2	<u>14.7</u> ±0.7	92.1 ±0.3	<u>25.6</u> ±1.0	91.3 ±0.2
CVaR	14.2 ±0.4	94.3 ±0.1	8.2 ±0.7	95.4 ±0.3	16.0 ±0.4	96.7
Chisq	12.1 ±0.2	95.8	9.5 ±0.5	95.0 ±0.2	13.6 ±0.7	97.0
CVaR_doro	9.6 ±0.2	<u>96.7</u>	5.9 ±0.1	96.7	14.5 ±0.3	96.1
Chisq_doro	13.0 ±0.1	95.3 ±0.1	<u>12.7</u> ±0.3	95.1 ±0.1	15.0 ±0.4	<u>97.4</u>
CVaR_group	12.7 ±0.3	95.8 ±0.1	9.3 ±0.2	96.0 ±0.1	<u>20.3</u> ±1.2	96.4 ±0.1
Variant	15.5 ±0.1	94.9 ±0.1	6.3 ±0.2	<u>97.7</u>	17.2 ±0.4	<u>97.7</u>
Group	14.3 ±0.4	95.3 ±0.1	8.9 ±0.4	96.3 ±0.2	12.9 ±0.5	96.5
Gradient	3.2 ±0.2	<u>98.6</u> ±0.1	2.6 ±0.1	<u>99.0</u>	14.3 ±1.0	95.7 ±0.1

Table 3: Performance Results for Various Methods in Real-World Datasets (In the table above, entries without a variance annotation indicate a variance of 0.0%. The blue single underline denotes the first place, the orange dotted underline indicates the second place, and the yellow double underline represents the third place.)

Method	Assay	Scaffold	Size
	Class 1(Max%)	Class 1(Max%)	Class 1(Max%)
ERM	20.3	9.3	23.5
ERM+NNR	20.3	14.9	24.2
ERM+CMO-KL	33.8	<u>31.5</u>	<u>38.3</u>
ERM+CMO-Chi	<u>41.6</u>	22.1	38.3
ERM+NNR+CMO-KL	<u>38.0</u>	<u>31.8</u>	<u>42.2</u>
ERM+NNR+CMO-Chi	<u>47.2</u>	<u>34.9</u>	<u>48.0</u>
CVaR	22.3	24.9	25.6
Chisq	18.0	22.1	27.4
CVaR_doro	15.1	10.0	20.2
Chisq_doro	17.4	21.1	22.7
CVaR_group	19.0	14.9	34.3
Variant	22.3	17.3	28.2
Group	24.6	24.6	24.5
Gradient	15.4	10.4	33.2

Table 4: Maximum value of the minority group for drugood_lbap_core_ki (The blue single underline denotes the first place, the orange dotted underline indicates the second place, and the yellow double underline represents the third place.)

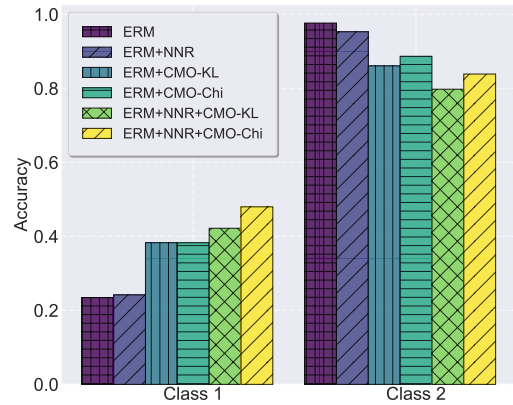


Figure 4: Performance on real-world dataset

results demonstrate that our methods effectively improve the generalization ability and robustness of graph models across diverse environments.

4.7 Hyperparameter Sensitive Analysis

To evaluate the influence of key hyperparameters- Γ , λ , and η_q -on the performance of our model, we conduct a sensitivity analysis by varying these hyperparameters within reasonable ranges. Specifically, Γ controls the distance metric in NNR, λ represent the coefficient of regularization terms in the update formulas (11), and η_q refers to the learning rate for the parameter q during optimization. The experimental results can be seen in 6.

5 Conclusion

In this work, we address the challenges of class imbalance and noise in Graph OOD learning by proposing CMO and NNR. Experimental

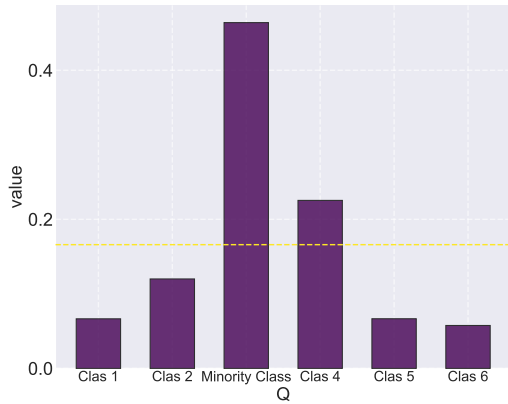


Figure 5: Q value of different classes, yellow line donates the initial weight of each class

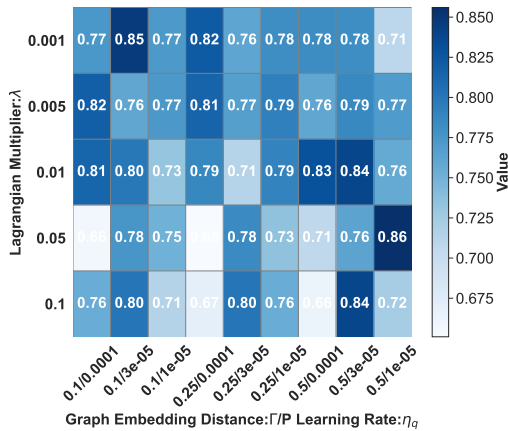


Figure 6: Performance on different hyperparameters

References

- [1] Rangachari Anand, Kishan G Mehrotra, Chilukuri K Mohan, and Sanjay Ranka. 1993. An improved algorithm for neural network classification of imbalanced training sets. *IEEE transactions on neural networks* 4, 6 (1993), 962–969.
- [2] Yongqiang Chen, Yatao Bian, Kaiwen Zhou, Binghui Xie, Bo Han, and James Cheng. 2023. Does Invariant Graph Learning via Environment Augmentation Learn Invariance?. In *NeurIPS*.
- [3] Hyeonmin Cho and Sangkyun Lee. 2021. Data quality measures and efficient evaluation algorithms for large-scale high-dimensional data. *Applied Sciences* 11, 2 (2021), 472.
- [4] Noel Cressie and Timothy RC Read. 1984. Multinomial goodness-of-fit tests. *Journal of the Royal Statistical Society Series B: Statistical Methodology* 46, 3 (1984), 440–464.
- [5] Hanjun Dai, Yichen Wang, Rakshit Trivedi, and Le Song. 2016. Deep coevolutionary network: Embedding user and item features for recommendation. *arXiv preprint arXiv:1609.03675* (2016).
- [6] Shaohua Fan, Xiao Wang, Yanhu Mo, Chuan Shi, and Jian Tang. 2022. Debiasing graph neural networks via learning disentangled causal substructure. In *NeurIPS*.
- [7] Dragan Gamberger, Nada Lavrac, and Ciril Groselj. 1999. Experiments with noise filtering in a medical domain. In *ICML*, Vol. 99. 143–151.
- [8] Cheng Hsu and Cheng-Te Li. 2021. Retagnn: Relational temporal attentive graph neural networks for holistic sequential recommendation. In *Proceedings of the web conference 2021*. 2968–2979.
- [9] Yuanfeng Ji, Lu Zhang, Jiaxiang Wu, Bingzhe Wu, Long-Kai Huang, Tingyang Xu, Yu Rong, Lanqing Li, Jie Ren, Ding Xue, Houtim Lai, Shaoyong Xu, Jing Feng, Wei Liu, Ping Luo, Shuigeng Zhou, Junzhou Huang, Peilin Zhao, and Yatao Bian. 2022. DrugOOD: Out-of-Distribution (OOD) Dataset Curator and Benchmark for AI-aided Drug Discovery – A Focus on Affinity Prediction Problems with Noise Annotations. *arXiv e-prints*, Article arXiv:2201.09637 (Jan. 2022), arXiv:2201.09637 pages. arXiv:2201.09637 [cs.LG]
- [10] Tianrui Jia, Haoyang Li, Cheng Yang, Tao Tao, and Chuan Shi. 2024. Graph Invariant Learning with Subgraph Co-mixup for Out-Of-Distribution Generalization. In *AAAI*.
- [11] Haoyang Li, Xin Wang, Ziwei Zhang, and Wenwu Zhu. 2022. Ood-gnn: Out-of-distribution generalized graph neural network. *IEEE Transactions on Knowledge and Data Engineering* 35, 7 (2022), 7328–7340.
- [12] Haoyang Li, Xin Wang, Ziwei Zhang, and Wenwu Zhu. 2022. Out-of-distribution generalization on graphs: A survey. *arXiv preprint arXiv:2202.07987* (2022).
- [13] Shuhan Liu and Kaize Ding. 2024. Beyond Generalization: A Survey of Out-Of-Distribution Adaptation on Graphs. *arXiv preprint arXiv:2402.11153* (2024).
- [14] Jiaqi Ma, Junwei Deng, and Qiaozhu Mei. 2021. Subgroup generalization and fairness of graph neural networks. *Advances in Neural Information Processing Systems* 34 (2021), 1048–1061.
- [15] Hongseok Namkoong and John C Duchi. 2016. Stochastic gradient methods for distributionally robust optimization with f-divergences. *Advances in neural information processing systems* 29 (2016).
- [16] Arkadi Nemirovski, Anatoli Juditsky, Guanghui Lan, and Alexander Shapiro. 2009. Robust stochastic approximation approach to stochastic programming. *SIAM Journal on optimization* 19, 4 (2009), 1574–1609.
- [17] Diana Pfau and Alexander Jung. 2024. Engineering Trustworthy AI: A Developer Guide for Empirical Risk Minimization. *arXiv preprint arXiv:2410.19361* (2024).
- [18] Shiori Sagawa, Pang Wei Koh, Tatsunori B Hashimoto, and Percy Liang. 2019. Distributionally robust neural networks for group shifts: On the importance of regularization for worst-case generalization. *arXiv preprint arXiv:1911.08731* (2019).
- [19] Bohao Wang, Jiawei Chen, Changdong Li, Sheng Zhou, Qihao Shi, Yang Gao, Yan Feng, Chun Chen, and Can Wang. 2024. Distributionally robust graph-based recommendation system. In *Proceedings of the ACM Web Conference 2024*. 3777–3788.
- [20] Hongxin Wei, Lue Tao, Renchunzi Xie, Lei Feng, and Bo An. 2022. Open-sampling: Exploring out-of-distribution data for re-balancing long-tailed datasets. In *International conference on machine learning*. PMLR, 23615–23630.
- [21] Man Wu, Xin Zheng, Qin Zhang, Xiao Shen, Xiong Luo, Xingquan Zhu, and Shirui Pan. 2024. Graph learning under distribution shifts: A comprehensive survey on domain adaptation, out-of-distribution, and continual learning. *arXiv preprint arXiv:2402.16374* (2024).
- [22] Qitian Wu, Fan Nie, Chenxiao Yang, Tianyi Bao, and Junchi Yan. 2024. Graph Out-of-Distribution Generalization via Causal Intervention. In *WWW*.
- [23] Qitian Wu, Hengrui Zhang, Junchi Yan, and David Wipf. 2022. HANDLING DISTRIBUTION SHIFTS ON GRAPHS: AN INVARIANCE PERSPECTIVE. In *ICLR*.
- [24] Rongling Wu and Libo Jiang. 2021. Recovering dynamic networks in big static datasets. *Physics Reports* 912 (2021), 1–57.
- [25] Ying-Xin Wu, Xiang Wang, An Zhang, Xiangnan He, and Tat-Seng Chua. 2022. DISCOVERING INVARIANT RATIONALES FOR GRAPH NEURAL NETWORKS. In *ICLR*.
- [26] Carl Yang, Aditya Pal, Andrew Zhai, Nikil Pancha, Jiawei Han, Charles Rosenberg, and Jure Leskovec. 2020. Multisage: Empowering gcn with contextualized multi-embeddings on web-scale multipartite networks. In *Proceedings of the 26th ACM SIGKDD international conference on knowledge discovery & data mining*. 2434–2443.
- [27] Jiaxuan You, Yichen Wang, Aditya Pal, Pong Eksombatchai, Chuck Rosenberg, and Jure Leskovec. 2019. Hierarchical temporal convolutional networks for dynamic recommender systems. In *The world wide web conference*. 2236–2246.
- [28] Runtian Zhai, Chen Dan, Zico Kolter, and Pradeep Ravikumar. 2021. Doro: Distributional and outlier robust optimization. In *International Conference on Machine Learning*. PMLR, 12345–12355.